

## Effects of Mg on the electrical characteristics and thermal stability of $\text{Mg}_x\text{Zn}_{1-x}\text{O}$ thin film transistors

Chieh-Jen Ku,<sup>1</sup> Ziqing Duan,<sup>1</sup> Pavel I. Reyes,<sup>1</sup> Yicheng Lu,<sup>1,a)</sup> Yi Xu,<sup>2</sup> Chien-Lan Hsueh,<sup>2</sup> and Eric Garfunkel<sup>2</sup>

<sup>1</sup>Department of Electrical and Computer Engineering, Rutgers University, Piscataway, New Jersey 08854, USA

<sup>2</sup>Department of Chemistry and Chemical Biology, Rutgers University, Piscataway, New Jersey 08854, USA

(Received 15 February 2011; accepted 25 February 2011; published online 25 March 2011)

The effects of the Mg composition ( $x=0, 0.06,$  and  $0.10$ ) on the electrical characteristics and thermal stability of  $\text{Mg}_x\text{Zn}_{1-x}\text{O}$  thin film transistors (TFTs) are investigated. The  $\text{Mg}_{0.06}\text{Zn}_{0.94}\text{O}$  TFT shows the smallest subthreshold slope and highest field effect mobility. The  $\text{O}_{1s}$  spectra of x-ray photoelectron spectroscopy measurements indicate that the oxygen vacancies are reduced in  $\text{Mg}_{0.06}\text{Zn}_{0.94}\text{O}$  relative to a pure ZnO channel device.  $\text{Mg}_{0.06}\text{Zn}_{0.94}\text{O}$  TFTs also show higher thermal stability compared to the pure ZnO TFTs, which is mainly attributed to the suppression of oxygen vacancies in the channel. © 2011 American Institute of Physics. [doi:10.1063/1.3567533]

Recently, ZnO thin film transistors (TFTs) have attracted increasing attention due to their high electron mobility, transparency to visible light, and superior radiation hardness. ZnO TFTs are potentially much less expensive than indium tin oxide based TFTs due to materials costs. It has been found that in ZnO based TFTs, the device characteristics, including field effect mobility, on-off ratio, subthreshold swing, and bias stress stability, are strongly impacted by the presence of native defects in the channel layer.<sup>1</sup> First principles calculation shows that the oxygen vacancy in ZnO has the lowest formation energy among the donorlike defects with deep electronic states.<sup>2</sup> Generally, an oxygen vacancy in the n-type ZnO is in the neutral state ( $V_o$ ). However, under the negative gate voltage, the band bending can create the electron depletion region in the TFT channel. In this region,  $V_o$  can be excited to doubly the ionized state ( $V_o^{2+}$ ) and releases electrons into the conduction band.<sup>3</sup> Thus, generation of  $V_o^{2+}$  from thermally excited  $V_o$  in the depletion region under a negative gate voltage increases the conductivity, resulting in the thermal instability of ZnO TFTs.

It has been reported that the incorporation of Mg into  $\text{HfO}_2$  effectively reduces oxygen vacancies.<sup>4</sup> Current understanding is that Mg becomes strongly bonded to oxygen vacancies ( $V_o^{2+}$ ) in  $\text{HfO}_2$ , neutralizing this defect. We speculate that the incorporation of certain metal ions (M) that have a stronger oxygen affinity than Zn in ZnO may also suppress the oxygen vacancies since the formation energy of oxygen vacancies depends in part on the M-O/Zn-O bonding energy. Mg might be a good candidate to serve as the oxygen vacancy suppressor in ZnO TFTs. First, the  $\text{Mg}^{2+}$  substitution in the  $\text{Zn}^{2+}$  site does not cause significant lattice distortion due to their similar ionic radii ( $\text{Mg}^{2+}$ : 0.57 Å versus  $\text{Zn}^{2+}$ : 0.60 Å). Second, owing to the strong ionic characteristic of MgO, the bonding energy of MgO (393.7 kJ/mole) is higher than ZnO (284.1 kJ/mol) at 298 K.<sup>5</sup> First principles calculations also indicates that MgO has a higher formation energy per oxygen vacancy (10.08 eV) than ZnO (7.01 eV).<sup>6</sup> It has been reported that alloying of Mg into ZnO can reduce

deep level luminescence associated with oxygen vacancies in both polycrystalline and epitaxial  $\text{Mg}_x\text{Zn}_{1-x}\text{O}$  films.<sup>7,8</sup> However, there has been little information on use of Mg alloying in ZnO to form  $\text{Mg}_x\text{Zn}_{1-x}\text{O}$  TFTs.

Ohtomo *et al.*<sup>9</sup> studied the photoresponse of  $\text{Mg}_x\text{Zn}_{1-x}\text{O}$  TFTs ( $x=0, 0.1,$  and  $0.3$ ). The field effect mobility was found to decrease from 2.7  $\text{cm}^2/\text{V s}$  for ZnO to 0.8  $\text{cm}^2/\text{V s}$  for  $\text{Mg}_{0.1}\text{Zn}_{0.9}\text{O}$  although no obvious structure change was found from x-ray diffraction. The degradation of the field effect mobility was attributed to the alloying disorder and increased effective mass of electrons.<sup>9,10</sup> Recently, Kim *et al.*<sup>11</sup> investigated how Mg alloying affects the bias stress stability of high indium content (molar ratio In:Zn = 9:1) sol-gel InZnO (IZO) TFTs with increasing Mg/(In + Zn) ratios up to 0.4. The improvement of the bias stress stability, resulting from incorporation of Mg into the IZO TFTs, was attributed to smoother surface morphology, a reduced size of voids both at the interface and in the film, and enlargement of the band gap.

In this letter, we investigate the effects of Mg alloying on the electrical characteristics and thermal stability of  $\text{Mg}_x\text{Zn}_{1-x}\text{O}$  TFTs ( $x \leq 0.1$ ).  $\text{Mg}^{2+}$  ions were incorporated to prevent oxygen out-diffusion and hinder the formation of oxygen vacancies in the TFT channel. The Mg composition is limited to no more than 10% to minimize deterioration of the field effect mobility. Bottom gate  $\text{Mg}_x\text{Zn}_{1-x}\text{O}$  TFTs were fabricated on heavily doped n-type Si wafers with a 100 nm thermally grown  $\text{SiO}_2$ . The 50 nm  $\text{Mg}_x\text{Zn}_{1-x}\text{O}$  ( $x=0, 0.06,$  and  $0.10$ ) channels are grown by metal-organic chemical vapor deposition at 450 °C. DEZn (diethyl zinc) and  $\text{MCP}_2\text{Mg}$  [bis (methylcyclopentadienyl) magnesium] are the precursors for Zn and Mg, respectively. The source and drain metallizations are formed with 100 nm Ti/50 nm Au by a lift-off process. The active layer is fixed at a width/length (W/L) = 150  $\mu\text{m}/5 \mu\text{m}$ . To prevent ambient absorption/desorption during the electrical testing, a SU-8 resist is coated on top of the TFT channel, serving as a passivation layer.<sup>12</sup> All the electrical tests are conducted in the dark using an HP-4156C electrical testing system with a temperature controlled chuck.

Figures 1(a) and 1(b) show the  $I_{\text{DS}}-V_{\text{GS}}$  characteristics in the linear and saturation regions for three TFTs with different

<sup>a)</sup>Author to whom correspondence should be addressed. Electronic mail: ylu@rci.rutgers.edu.

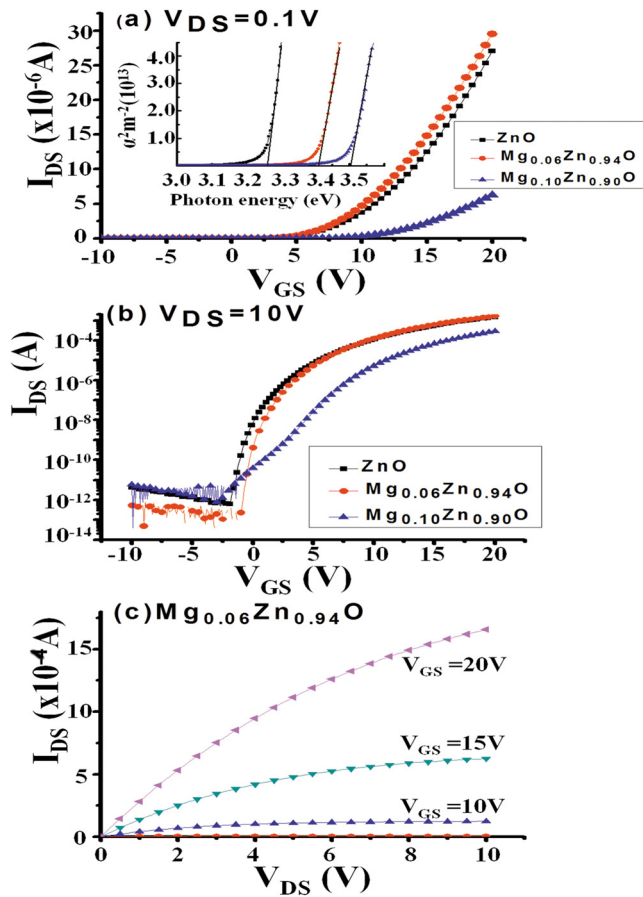


FIG. 1. (Color online)  $I_{DS}$ - $V_{GS}$  transfer characteristics of ZnO,  $Mg_{0.06}Zn_{0.94}O$ , and  $Mg_{0.1}Zn_{0.9}O$  TFTs: (a) in the linear region; the inset shows the  $\alpha^2$  vs  $h\nu$  curves of ZnO,  $Mg_{0.06}Zn_{0.94}O$  and  $Mg_{0.1}Zn_{0.9}O$ ; (b) in the saturation region; and (c) the  $I_{DS}$ - $V_{DS}$  characteristics of  $Mg_{0.06}Zn_{0.94}O$  TFTs.

Mg concentrations. The Mg composition values  $x$  in the  $Mg_xZn_{1-x}O$  are extracted from the absorption curves ( $\alpha^2$  versus  $h\nu$ ), as shown in the inset of Fig. 1(a). The field effective mobilities of these three TFTs are extracted from the linear region. All of the TFTs show high on-off ratios ( $>10^9$ ). The extracted threshold voltages ( $V_{th}$ ) for ZnO,  $Mg_{0.06}Zn_{0.94}O$ , and  $Mg_{0.1}Zn_{0.9}O$  TFTs are 2.1 V, 3.5 V, and 4.5 V, respectively. For the ZnO TFT, a field effect mobility  $\mu_{FE}$  of  $30 \text{ cm}^2/\text{V s}$  and a subthreshold swing  $S$  of  $0.54 \text{ V/dec}$  are obtained. Severe degradation of mobility ( $\mu_{FE}=8 \text{ cm}^2/\text{V s}$ ) and subthreshold swing ( $S=1.9 \text{ V/dec}$ ) is observed for the  $Mg_{0.1}Zn_{0.9}O$  TFT, resulted from alloying disorder and an increased effective mass of the electrons.<sup>9</sup> However, in contrast to the high Mg composition (10%) case, the  $Mg_{0.06}Zn_{0.94}O$  TFT shows the highest field effect mobility ( $\mu_{FE}=40 \text{ cm}^2/\text{V s}$ ) and lowest subthreshold swing ( $S=0.25 \text{ V/dec}$ ). Figure 1(c) shows the hard saturation behavior in the  $I_{DS}$ - $V_{DS}$  curve. The maximum bulk trap density ( $N_{BS}$ ) in the channel can be extracted from the subthreshold swing value,  $S$ :<sup>13</sup>  $S=(kT/q) \times \log_e 10 \times [1+qtN_{BS}/C_{ins}]$ , where  $k$  is the Boltzmann constant,  $T$  is the temperature,  $q$  is the elementary charge,  $t$  is the thickness of the channel, and  $C_{ins}$  is the capacitance of insulator. The extracted values of  $N_{BS}$  for ZnO and  $Mg_{0.06}Zn_{0.94}O$  TFTs are  $3.53 \times 10^{17} \text{ cm}^{-3}$  and  $1.37 \times 10^{17} \text{ cm}^{-3}$ , respectively. The decrease in bulk trap density indicates that the electron traps associated with oxy-

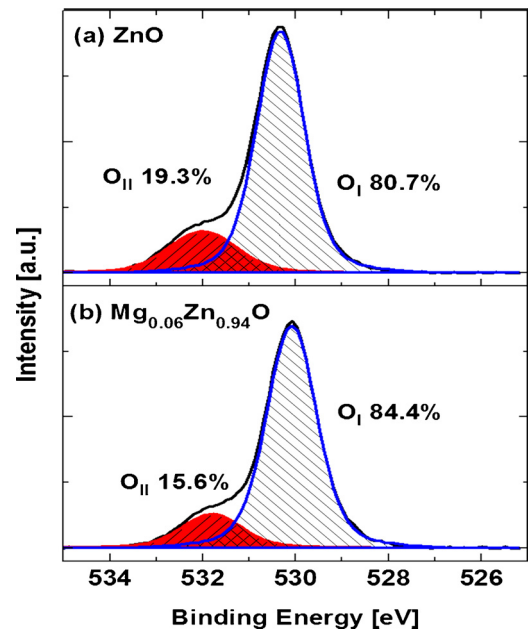


FIG. 2. (Color online) The  $O_{1s}$  peaks in the XPS spectra of (a) pure ZnO and (b)  $Mg_{0.06}Zn_{0.94}O$  channel layers. The original  $O_{1s}$  peaks were deconvoluted by Gaussian fitting into two subpeaks including  $O_I$  (oxygen bonded with Zn) and  $O_{II}$  (oxygen vacancy related). The peak area of  $O_{II}/(O_I+O_{II})$  is reduced after incorporation of 6% Mg into the ZnO.

gen vacancies in the ZnO channel are reduced<sup>13</sup> after alloying of 6% Mg to form  $Mg_{0.06}Zn_{0.94}O$ .

Figures 2(a) and 2(b) show  $O_{1s}$  peaks in x-ray photoelectron spectroscopy (XPS) spectra of ZnO and  $Mg_{0.06}Zn_{0.94}O$  thin films, respectively. Gaussian fitting is used in the deconvolution of these  $O_{1s}$  peaks. The peak at the lower binding energy  $\sim 530 \text{ eV}$  ( $O_I$ ) is attributed to  $O^{2-}$  ions present in a stoichiometric wurtzite ZnO structure, whereas the peak at the higher binding energy  $\sim 532 \text{ eV}$  ( $O_{II}$ ) has been attributed to  $O^{2-}$  ions in “oxygen deficient” ZnO.<sup>14</sup> The ratio of peak area ( $O_{II}/O_{tot}$ ), indicating the relative quantity of this oxygen-related defect, is reduced from 19.3% (for ZnO) to 15.6% (for  $Mg_{0.06}Zn_{0.94}O$ ) after 6% Mg is alloying into the ZnO thin film. Also, the  $O_I/O_{II}$  peak positions shifted to lower binding energies from  $530.32/532.08$  to  $530.08/531.80 \text{ eV}$  due to a decrease in the number of oxygen vacancies.

Figures 3(a) and 3(b) illustrate the evolution of the transfer characteristics of ZnO and  $Mg_{0.06}Zn_{0.94}O$  TFTs at different temperatures, ranging from 300 to 375 K. Both TFTs exhibit a negatively shifted threshold voltage  $V_{th}$  with increasing temperature:  $\Delta V_{th}$  of ZnO TFT and  $Mg_{0.06}Zn_{0.94}O$  TFT are 1.5 V and 0.5 V, respectively. The subthreshold drain current of ZnO TFT increases from  $2.2 \times 10^{-10}$  to  $8.6 \times 10^{-8} \text{ A}$  with a  $V_{GS}$  of  $-2 \text{ V}$ . In contrast to the ZnO TFT, the subthreshold drain current of  $Mg_{0.06}Zn_{0.94}O$  TFT only increases from  $2.3 \times 10^{-10}$  to  $8.0 \times 10^{-9} \text{ A}$  with a  $V_{GS}$  of  $1.5 \text{ V}$ . Under a negative gate voltage, neutral oxygen vacancies ( $V_o$ ) in the depletion region of ZnO channel can be thermally excited to ionized state ( $V_o^{2+}$ ). Ionized oxygen vacancies would release electrons into the conduction band. The higher channel conductivity and lower  $V_{th}$  are induced by the formation of ionized oxygen vacancies. The simulation of the depletion width for deep traps at high concentration<sup>15</sup> shows that with a negative gate voltage of 5 V, the entire channel of the ZnO TFT can be fully depleted under the assumption of trap density  $N_T=10^{16}-10^{18} \text{ cm}^{-3}$ .

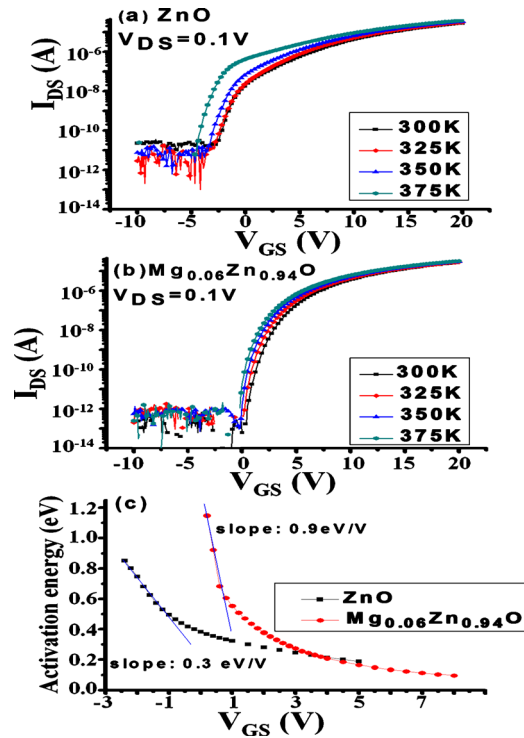


FIG. 3. (Color online) The evolution of transfer characteristics of (a) ZnO TFT and (b)  $\text{Mg}_{0.06}\text{Zn}_{0.94}\text{O}$  TFT at different temperatures, ranging from 300 to 375 K. (c) The extracted activation energies as a function of  $V_{\text{GS}}$  for ZnO and  $\text{Mg}_{0.06}\text{Zn}_{0.94}\text{O}$  TFTs.

The activation energy of the drain current extracted from an Arrhenius plot is used to approximately track the position of Fermi level ( $E_A = E_C - E_F$ ) in the band gap. Figure 3(c) shows the activation energy ( $E_A$ ) of the drain current as a function of  $V_{\text{GS}}$ . The maximum activation energy of ZnO TFT is 0.85 eV while for  $\text{Mg}_{0.06}\text{Zn}_{0.94}\text{O}$  TFT it is 1.15 eV. The increase in activation energy of  $\text{Mg}_{0.06}\text{Zn}_{0.94}\text{O}$  TFT cannot be explained only by the increase in the energy band gap since the optical band gap only increases by  $\sim 0.15$  eV. The higher energy barrier of  $\text{Mg}_{0.06}\text{Zn}_{0.94}\text{O}$  TFT may result from the stronger bonding of Mg-O as compared to Zn-O, meaning that the formation of oxygen vacancies is suppressed and the density of oxygen vacancies is also reduced. In addition, the activation energy ( $E_A$ ) of the  $\text{Mg}_{0.06}\text{Zn}_{0.94}\text{O}$  TFT decreases faster as a function of  $V_{\text{GS}}$ . The falling rate of  $E_A$  with respect to  $V_{\text{GS}}$  is correlated with the filling of traps in the active layer and the gate insulator/active layer interface.<sup>16</sup> For a TFT with a large trap density ( $N_{\text{tot}}$ ), the decrease in  $E_A$  with  $V_{\text{GS}}$  is approximately inversely proportional to the  $N_{\text{tot}}$ . Because all TFTs are fabricated on the same thermally grown  $\text{SiO}_2/\text{Si}$  film, it can be presumed that most of the contribu-

tion of  $N_{\text{tot}}$  comes from bulk trap density ( $N_{\text{BS}}$ ) of the channel. The faster decrease in  $E_A$  (0.9 eV/V) with respect to  $V_{\text{GS}}$  in the  $\text{Mg}_{0.06}\text{Zn}_{0.94}\text{O}$  TFT compared to ZnO TFT (0.3 eV/V) suggests that the  $N_{\text{tot}}$  in  $\text{Mg}_{0.06}\text{Zn}_{0.94}\text{O}$  TFT is diminished by roughly three times relative to a ZnO TFT. This inference is consistent with the value of  $N_{\text{BS}}$  extracted from the subthreshold slope. Thus, the improved thermal stability and electrical characteristics of  $\text{Mg}_{0.06}\text{Zn}_{0.94}\text{O}$  TFT can be mainly attributed to a reduced density of oxygen vacancies and the associated electron traps by incorporation of Mg ions into ZnO.

In summary, with 6% Mg incorporation into a ZnO channel, the field effect mobility and subthreshold swing values are improved. A smaller (negative) shift of threshold voltage and higher activation energy are observed. The improved electrical characteristics and thermal stability of  $\text{Mg}_{0.06}\text{Zn}_{0.94}\text{O}$  TFT are mainly attributed to the suppression of oxygen vacancies by introducing stronger Mg-O bonding in the channel layer.

The authors would like to thank Dr. D. C. Look for his insightful and valuable suggestion. This project has been supported by the AFOSR under Grant No. FA9550-08-01-0452 and by the NSF under Grant No. ECCS1002178.

- <sup>1</sup>C. T. Tsai, T. C. Chang, S. C. Chen, I. Lo, S. W. Tsao, M. C. Hung, J. J. Chang, and C. Y. Huang, *Appl. Phys. Lett.* **96**, 242105 (2010).
- <sup>2</sup>A. F. Kohan, G. Ceder, D. Morgan, and C. G. Van de Walle, *Phys. Rev. B* **61**, 15019 (2000).
- <sup>3</sup>K. Vanheusden, C. H. Segar, W. L. Warren, D. R. Tallant, and J. A. Viogt, *Appl. Phys. Lett.* **68**, 403 (1996).
- <sup>4</sup>N. Umezawa, M. Sato, and K. Shiraiishi, *Appl. Phys. Lett.* **93**, 223104 (2008).
- <sup>5</sup>Y. Yao and T. Xie, *The Handbook of Physics and Chemistry* (CRC Press, Boca Raton, FL, 1985), Vol. 111.
- <sup>6</sup>J. Carrasco, N. Lopez, and F. Illas, *Phys. Rev. Lett.* **93**, 225502 (2004).
- <sup>7</sup>F. K. Shan, B. I. Kim, G. X. Liu, Z. F. Liu, J. Y. Sohn, W. J. Lee, B. C. Shin, and Y. S. Yu, *J. Appl. Phys.* **95**, 4772 (2004).
- <sup>8</sup>A. K. Sharma, J. Narayan, J. F. Muth, C. W. Teng, C. Jin, A. Kvit, R. M. Kolbas, and O. W. Holland, *Appl. Phys. Lett.* **75**, 3327 (1999).
- <sup>9</sup>A. Ohtomo, S. Takagi, K. Tamura, T. Makino, Y. Segawa, H. Koinuma, and M. Kawasaki, *Jpn. J. Appl. Phys., Part 2* **45**, L694 (2006).
- <sup>10</sup>K. Matsubara, H. Tampo, H. Shibata, A. Yamada, P. Fons, K. Iwata, and S. Niki, *Appl. Phys. Lett.* **85**, 1374 (2004).
- <sup>11</sup>G. H. Kim, W. H. Jeong, B. D. Ahn, H. S. Shin, H. J. Kim, H. J. Kim, M. K. Ryu, K. B. Park, J. B. Seon, and S. Y. Lee, *Appl. Phys. Lett.* **96**, 163506 (2010).
- <sup>12</sup>A. Olziersky, P. Barquinha, A. Vila, L. Pereira, G. Goncalves, E. Fortunato, R. Matins, and J. R. Morante, *J. Appl. Phys.* **108**, 064505 (2010).
- <sup>13</sup>K. Nomura, T. Kayami, H. Ohta, M. Hirano, and H. Hosono, *Appl. Phys. Lett.* **93**, 192107 (2008).
- <sup>14</sup>Y. S. Rim, D. L. Kim, W. H. Jeong, and H. J. Kim, *Appl. Phys. Lett.* **97**, 233502 (2010).
- <sup>15</sup>D. C. Look and J. R. Sizelove, *J. Appl. Phys.* **78**, 2848 (1995).
- <sup>16</sup>K. Takechi, M. Nakata, T. Eguchi, H. Yamaguchi, and S. Kaneko, *Jpn. J. Appl. Phys., Part 1* **48**, 011301 (2009).